

<https://doi.org/10.1038/s43247-024-01387-7>

Large variation in carbon dioxide emissions from tropical peat swamp forests due to disturbances

Check for updates

Takashi Hirano¹✉, Shinjiro Ohkubo^{1,2}, Masayuki Itoh^{3,4}, Hayato Tsuzuki⁵, Ayaka Sakabe⁶, Hidenori Takahashi⁷, Kitso Kusin⁸ & Mitsuru Osaki¹

The huge carbon stock of tropical peat swamp forest (PSF) in Southeast Asia has been threatened by environmental disturbances due to quasi-periodic El Niño-Southern Oscillation (ENSO) droughts, biomass and peat burning, smoke haze, drainage, and deforestation. Carbon dioxide (CO₂) emissions from such disturbances have not been well quantified because of insufficient field data. Therefore, we quantified the ecosystem-scale CO₂ balance and examine the disturbance effects from a long-term field experiment for 12–15 years at three PSF sites with different degrees of degradation in Indonesia. Here, we show a drastic change of an undrained PSF from a CO₂ sink to a source owing to the transient groundwater lowering by the droughts, a significant decrease in ecosystem photosynthesis due to the radiation attenuation by smoke haze in drought years, and long-lasting CO₂ emissions through enhanced peat decomposition by drainage. The impact on CO₂ emissions was greater from drainage than drought-induced disturbances.

A huge amount of soil carbon has accumulated over millennia, coexisting with peat swamp forest (PSF) in insular Southeast Asia¹. However, land conversion from PSF to plantations has accelerated since the 1990s, and agricultural land use with drainage covered 50% of the peatlands of Peninsular Malaysia, Sumatra, and Borneo (15.7 Mha) in 2015². In addition, PSFs degraded by logging and drainage were left in 23% of the peatland area². Another study³ reported that drainage occurred in at least 65% of peatlands in Southeast Asia. Land conversion and forest degradation lower groundwater levels (GWL) and enhance oxidative peat decomposition⁴, resulting in extensive carbon dioxide (CO₂) emissions^{5,6}. To assess peat CO₂ emissions at national and regional scales, the IPCC method⁷, in which CO₂ emissions are calculated as the product of the area of each land-use category and the corresponding Tier 1 emission factor (EF), has been commonly used^{5,6,8}. Although simple and practical, this method excludes spatio-temporal variations in GWL, transitional variations in peat oxidation after drainage, and CO₂ uptake through biomass growth^{7,9}. Peat decomposition rates strongly depend on GWL^{4,10,11} and show a decreasing trend over time after drainage^{12–14}. Moreover, vegetation's CO₂ uptake (photosynthesis) and emissions (respiration) must be quantified to assess the CO₂ balance of the ecosystem⁹.

El Niño-Southern Oscillation (ENSO) events cause drought every few years^{15,16}, leading to a sharp drop in GWL, even in undrained PSF^{17,18}. Therefore, drought enhances peat oxidation⁴ and increases the risk and severity of wildfires, which immediately emit large amounts of CO₂ through the combustion of biomass and peat^{19,20}. A wildfire burns the ecosystem at various levels depending on the intensity and duration of the fire and consequently changes ecosystem functions²¹. In addition, smoke emitted during fires disturbs the radiation environment, resulting in the attenuation of solar radiation and an increase in the diffuse radiation fraction^{22,23}. We reported the disturbance effects on the ecosystem-scale CO₂ balance (net ecosystem CO₂ exchange: NEE) of PSFs by comparing the eddy CO₂ flux measured simultaneously at three sites of almost undrained (UF), drained by a large canal (DF), and repeatedly burned (DB) PSFs in Central Kalimantan, Indonesia, using 4–6-year-long data until 2009¹⁷. However, the previous study should be updated using a longer dataset to detect the long-term effects of drainage and robustly quantify the disturbance effects. Therefore, we report updated findings on the effects on annual NEE, which is almost equivalent to CO₂ EF for unmanaged forests, of 1) transient GWL lowering by the ENSO droughts, 2) radiation attenuation by smoke haze, 3) persistent GWL lowering by drainage, and 4) repeated vegetation burning

¹Research Faculty of Agriculture, Hokkaido University, Sapporo, Japan. ²Forestry Research Institute, Hokkaido Research Organization, Bibai, Japan. ³School of Human Science and Environment, University of Hyogo, Himeji, Japan. ⁴Research Institute for Sustainable Humanosphere, Kyoto University, Uji, Japan. ⁵Faculty of Agriculture, Ehime University, Matsuyama, Japan. ⁶Graduate School of Agriculture, Kyoto University, Kyoto, Japan. ⁷Hokkaido Institute of Hydro-climate, Sapporo, Japan. ⁸University of Palangkaraya, Palangkaraya, Indonesia. ✉e-mail: hirano@agr.hokudai.ac.jp

from a long-term field experiment of 12–15 years at the three sites (Supplementary Fig. 1).

The UF drastically changed from a CO₂ sink in normal years to a large source in dry years caused by the ENSO droughts. The large change in an annual NEE (22.6 ± 14.6 Mg CO₂ ha⁻¹ yr⁻¹; mean \pm 1 standard deviation (SD)) was attributed to an increase in ecosystem respiration (RE) due to enhanced peat decomposition by transient GWL lowering and decreases in gross primary production (GPP) due to stomatal limitation by a water deficit and radiation attenuation by smoke haze; smoke haze contributed more to the GPP decrease than a water deficit did. The DF was a CO₂ source even in normal years owing to persistent GWL lowering by drainage. The difference in annual NEE between the DF and UF indicates that annual CO₂ emissions due to drainage was 15.2 ± 6.43 Mg CO₂ ha⁻¹ yr⁻¹ over the 20 years after canal excavation. Considering the occurrence frequency of the normal and dry years, the additional CO₂ emissions by drainage were 1.6 times greater than those by droughts during the common measurement period. At the DB, a large amount of CO₂ was emitted suddenly through biomass burning in 2009. On average, the effect of repeated burning on CO₂ emissions, which was estimated as the difference in annual NEE between the DB and UF, was almost equivalent to that of drainage.

Results and discussion

Carbon dioxide balance of the undrained forest

Mean annual precipitation was 2557 ± 432 mm yr⁻¹ (\pm 1 SD) between 2002 and 2018, and the annual number of dry months (monthly precipitation < 100 mm) was 2.6 ± 1.2 months yr⁻¹, indicating that the study site is a tropical rainforest or humid forest²⁴. Monthly precipitation showed a general seasonal pattern with a decrease in July–October¹⁵; consequently, the GWL showed a similar seasonal pattern (Supplementary Fig. 2). At the DF, the GWL remained belowground even during the wet season because of drainage.

The mean annual NEE of the undrained UF for 2005–2017 was -1.00 ± 13.2 Mg CO₂ ha⁻¹ yr⁻¹ with a random uncertainty of 0.70 ± 0.073 Mg CO₂ ha⁻¹ yr⁻¹, indicating the UF was a small CO₂ sink with a mean annual GWL of -0.15 ± 0.12 m (Supplementary Table 1). In contrast, an intact PSF in Riau, Indonesia⁹ was a strong source of 15.3 ± 3.70 Mg CO₂ ha⁻¹ yr⁻¹ with a mean annual GWL of -0.24 ± 0.22 m, whereas a secondary PSF in Sarawak, Malaysia²⁵ was a larger sink of -4.99 ± 1.87 Mg CO₂ ha⁻¹ yr⁻¹ with a mean annual GWL of -0.19 ± 0.03 m.

Drought effect

To examine drought effects, the experimental period of 2002–2018 was classified based on the annual dry-period length (DPL)²⁶ into seven dry, seven normal, and three wet years (Supplementary Table 2); the dry and wet

years were linked to El Niño and La Niña events, respectively. The two wet years (2010 and 2016) occurred in the years following strong droughts of 2009 and 2015, respectively. In the dry years, the GWL was much lower during the dry season and even in November and December after the rainy season began (Supplementary Fig. 3).

Annual CO₂ flux data of the undrained UF from 2005 to 2017 (Supplementary Table 1) were compared among the year types to detect drought effect. The UF was a CO₂ sink in the normal and wet years (-9.52 ± 6.93 and -2.79 ± 6.99 Mg CO₂ ha⁻¹ yr⁻¹, respectively) but a large source (13.1 ± 12.9 Mg CO₂ ha⁻¹ yr⁻¹) in the dry years (Fig. 1). In the dry years (GWL = -0.30 ± 0.07 m), the UF emitted an additional net CO₂ emission of 22.6 Mg CO₂ ha⁻¹ yr⁻¹ compared with the normal years (GWL = -0.08 ± 0.05 m). The large source was due to the significantly larger RE and smaller GPP in the dry years (Fig. 1). The large RE was caused by a lower GWL (Fig. 1) and its resultant enhancement of peat decomposition^{4,10,27}. The annual RE and NEE linearly increased as GWL decreased, respectively (Fig. 2). Apart from haze effect (described later), the small GPP was attributed to a smaller GPP₀ (light-saturated GPP without a vapor pressure deficit (VPD) limitation²⁸) (Fig. 1). GPP₀ showed a decreasing tendency as GWL decreased when GWL was lower than a threshold ($= -0.7$ m for UF) (Supplementary Fig. 4). In addition, the reference surface conductance^{29,30} ($G_{s,ref}$), which mainly depends on stomatal opening, showed a similar decreasing tendency at low GWL (Supplementary Fig. 5). Therefore, the decreased annual GPP in the dry years was partly caused by stomatal limitation due to a water deficit from lower GWL and higher VPD (Supplementary Fig. 3). In contrast, smaller GPP and GPP₀ values in the wet years (Fig. 1) were probably due to sustained damage from severe drought in previous years (2009 and 2015). Monthly GPP continued to decrease after drought for approximately one year, even in the wet season (Supplementary Fig. 3), resulting in a small net primary production (NPP = 2.53 ± 4.66 Mg C ha⁻¹ yr⁻¹) with no biomass increment at the UF in 2016 (Supplementary Table 3).

Smoke haze effect

Fire occurs around the study site in the dry season almost every year³¹ except for wet years³² (Supplementary Fig. 2). During dry years, fires spread widely and emit a large amount of smoke³³. The smoke haze diffuses and attenuates solar radiation³² (Fig. 3). Although diffuse radiation increases the light-use efficiency of forest GPP^{34,35}, smoke shading affects GPP negatively. Radiation attenuation is an artificial disturbance because fires are mostly ignited by people in Southeast Asia³⁶. The duration of smoke haze was found to be half a month to two months during three months from September to November, based on the time series of daily photosynthetic photon flux density (PPFD)

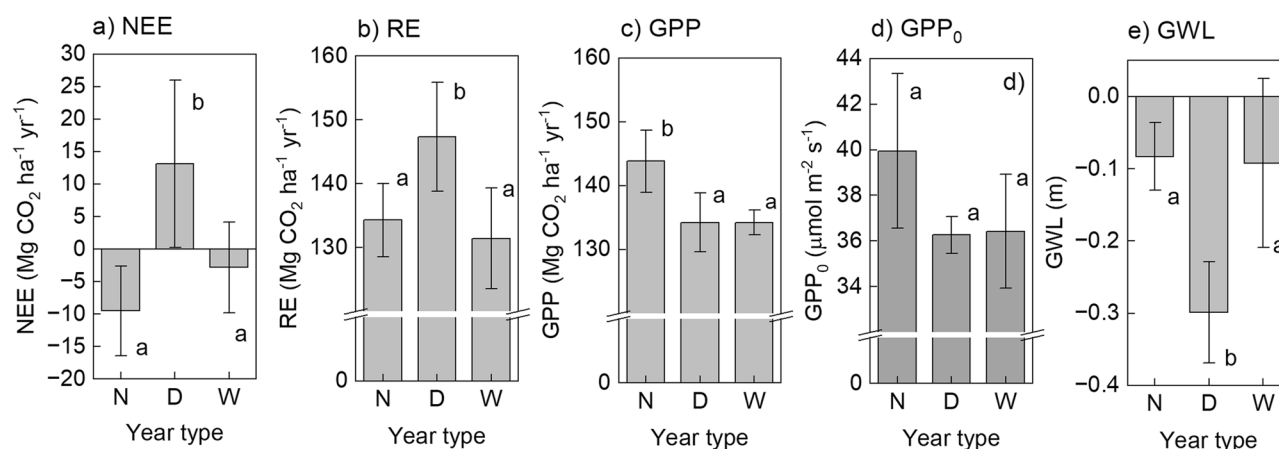


Fig. 1 | Comparison of annual gap-filled CO₂ fluxes and GWL at the UF site among the normal (N), dry (D), and wet (W) years. a NEE, **b** RE, **c** GPP, **d** light-saturated GPP (GPP) without the limitation of vapor pressure deficit (VPD), and **e** GWL. The normal years were 2005, 2007, 2008, 2011, and 2012; the dry years were

2006, 2009, 2014, and 2015; and the wet years were 2010, 2016, and 2017. Error bars denote 1 standard deviation. Different letters in each panel denote significant differences among the year types at significant levels of 0.05, according to Tukey's HSD.

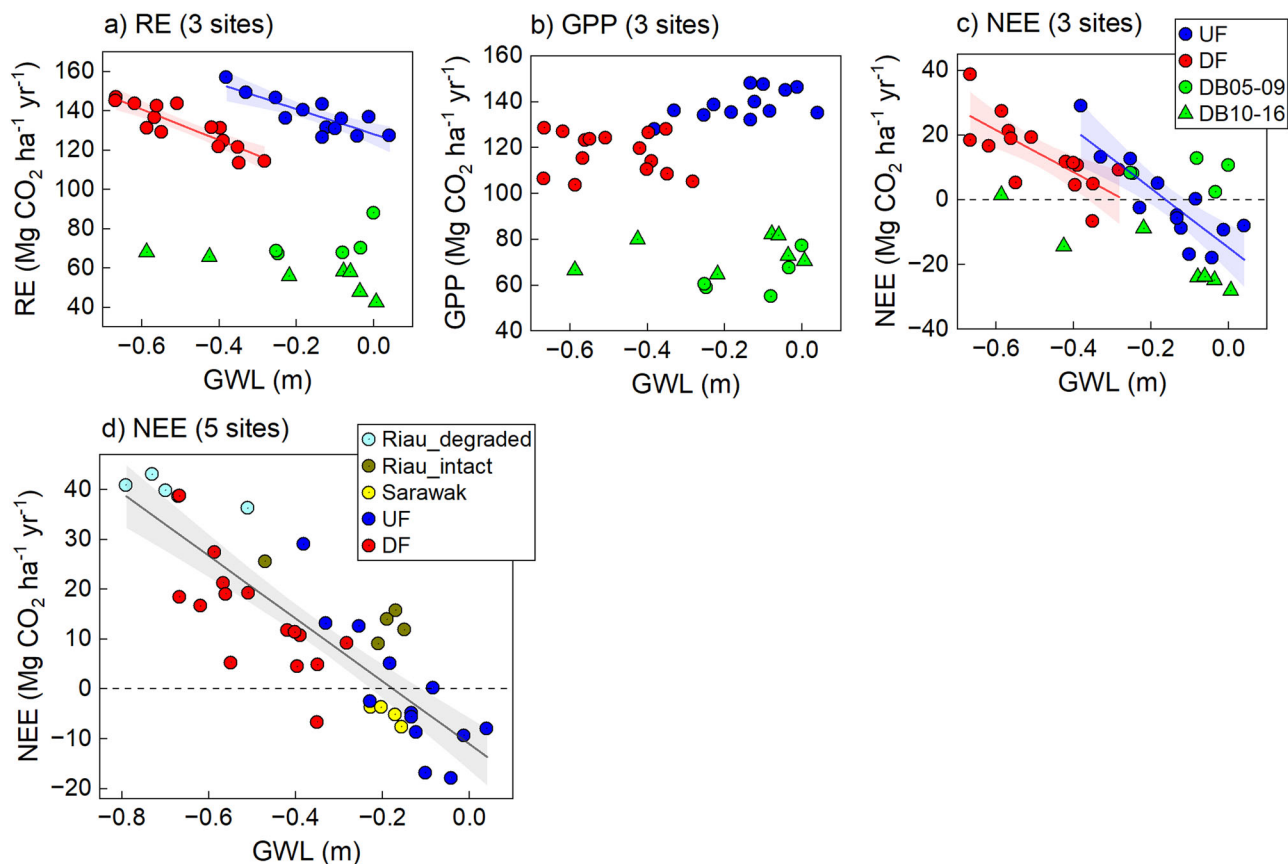


Fig. 2 | Relationships of annual gap-filled CO₂ fluxes with annual mean GWL at the UF, DF, and DB. **a** RE, **b** GPP, and **c** NEE. DB data were separated into two periods ending in 2009 and starting in 2010, because a fire occurred in 2009. Significant regression lines are drawn for RE for UF (RE = -63.9 GWL + 128, $R = 0.65$, $P < 0.001$), RE for DF (RE = -78.5 GWL + 93.6, $R = 0.75$, $P < 0.0001$), NEE for UF (NEE = -91.4 GWL + 14.8, $R = 0.69$, $P < 0.0001$), and NEE for DF (NEE = -64.8

GWL + 17.5, $R = 0.52$, $P = 0.015$). **d** NEE at the UF and DF are also plotted along with literature data (degraded and intact peat swamp forests in Riau, Indonesia and a secondary peat swamp forest in Sarawak, Malaysia). A significant regression line is drawn (NEE = -63.0 GWL - 11.1, $R = 0.71$, $P < 0.0001$). Shadows denote the 95% intervals.

and diffuse radiation fractions. During the three months, the PPFd, diffuse fraction, and midday VPD were significantly lower by 16%, higher by 15%, and higher by 12%, respectively, in the dry years (Fig. 3).

The cumulative GPP at the UF during the three months was significantly lower in the dry years (D1: 29.8 ± 3.85 Mg CO₂ ha⁻¹) than in the normal years (N: 36.3 ± 2.05 Mg CO₂ ha⁻¹) (Fig. 3). The difference of 6.49 Mg CO₂ ha⁻¹ for the three months was almost comparable to the difference in annual GPP (9.61 Mg CO₂ ha⁻¹ year⁻¹) between dry and normal years (Fig. 1). To separate the effects of radiation attenuation and dryness on the GPP decrease, dry years' GPP under no-haze conditions was simulated from the measured half-hourly VPD and GWL in each dry year and half-hourly PPFd averaged for normal years using a light curve parameterized for normal years (Methods). The simulation resulted in a cumulative GPP of 34.8 ± 1.10 Mg CO₂ ha⁻¹ (D2). Thus, GPP decrease due to radiation attenuation (haze) and dryness (water deficit) were estimated to be 5.04 (=34.8-29.8) and 1.43 (=36.3-34.8) Mg CO₂ ha⁻¹, respectively; the 5.04 Mg CO₂ ha⁻¹ accounts for 3.5% of annual GPP in the normal year (Fig. 1). The light-use efficiency of GPP (α in Eq. (1)) increased as GWL decreased when GWL was lower than -1 m (Supplementary Fig. 4). The higher light-use efficiency at low GWL was attributed to higher diffuse radiation fractions caused by smoke haze (Fig. 3). However, the negative effect of smoke shading on GPP was more than the positive effect of higher light-use efficiency.

Drainage effect

Drainage has expanded to at least 65% of Southeast Asian peatlands³. In the short term, drainage affects the peatland CO₂ balance in the same manner as

drought does. However, the drainage effect lasts for a long period. We examined the long-term effects of drainage by comparing the annual CO₂ fluxes between the drained DF and undrained UF (Supplementary Table 2).

Over the common measurement period of 2005–2016, the DF was a large CO₂ source (12.9 ± 11.9 Mg CO₂ ha⁻¹ yr⁻¹), whereas the UF was a small sink (-1.52 ± 13.6 Mg CO₂ ha⁻¹ yr⁻¹) (Supplementary Table 1). Annual RE was significantly larger at the UF by 7.85 ± 8.56 Mg CO₂ ha⁻¹ year⁻¹, even with higher GWL (Supplementary Fig. 6), probably because of larger autotrophic respiration arising from larger biomass (Supplementary Table 3). Soil chamber studies conducted at the same sites showed that soil respiration including root respiration was higher at the UF³⁷, but soil CO₂ emissions through peat decomposition was higher at the DF³⁸. The mean annual GWL was significantly lower at the DF (-0.46 ± 0.13 m) than the UF (-0.15 ± 0.13 m) (Supplementary Table 1), but the inter-site difference decreased with time at a rate of 1.46 cm yr⁻¹ (Supplementary Fig. 7). Subsidence due to drainage³⁹ and natural sedimentation in the unmanaged large canal (Supplementary Fig. 1) would have raised the GWL at the DF. According to the GWL rise, the inter-site RE difference (DF - UF) linearly increased in a negative direction (Supplementary Fig. 8), indicating that the RE decrease at the DF owing to less peat decomposition.

The annual GPP was significantly smaller at the DF by 22.3 ± 8.83 Mg CO₂ ha⁻¹ yr⁻¹ (Supplementary Fig. 6). The smaller GPP was mainly due to lower leaf area index (LAI); the LAI of the DF accounted for 76–84% of the UF in 2013–2016 (Supplementary Table 3). The DF forest seemed to acclimate to drainage to some extent^{38,40,41} because surface conductance ($G_{s,ref}$), which is mainly controlled by stomatal opening, remained high until a lower GWL than at the UF (Supplementary Fig. 5). Although the initial

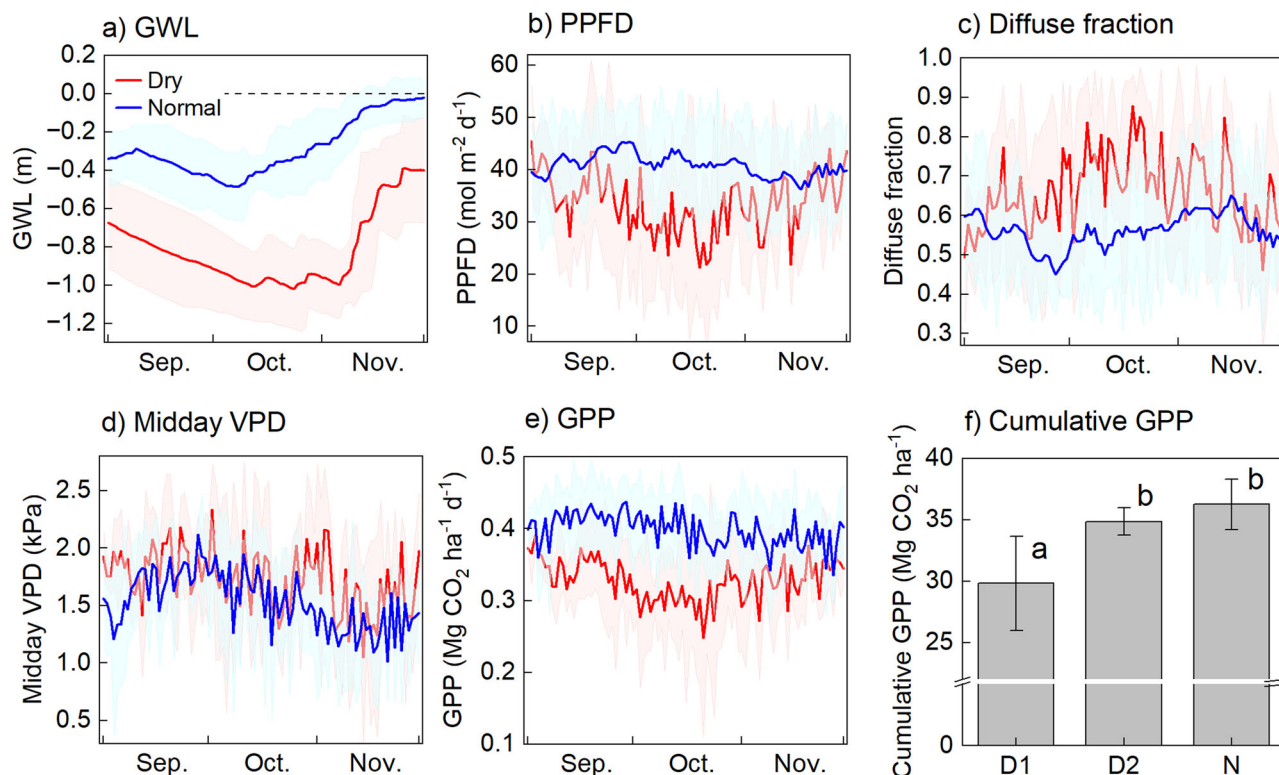


Fig. 3 | Comparison of mean daily variations at the UF between the normal (2005, 2007, 2008, 2011, 2012, and 2013) and dry (2006, 2009, 2014, and 2015) years for three months from September to November. a GWL, **b** PPFD, **c** diffuse solar radiation fraction, **d** midday (10–14 h) VPD, and **e** GPP. Shadows denote 1 standard deviation (SD). In addition, **f** cumulative GPP values for the three months

(mean ± 1 SD) were compared (D1: measured GPP after gap filling in the dry years, D2: simulated GPP in the dry years without smoke haze, and N: measured GPP after gap filling in the normal years). Different letters denote significant difference at significant levels of 0.05 according to Tukey’s HSD.

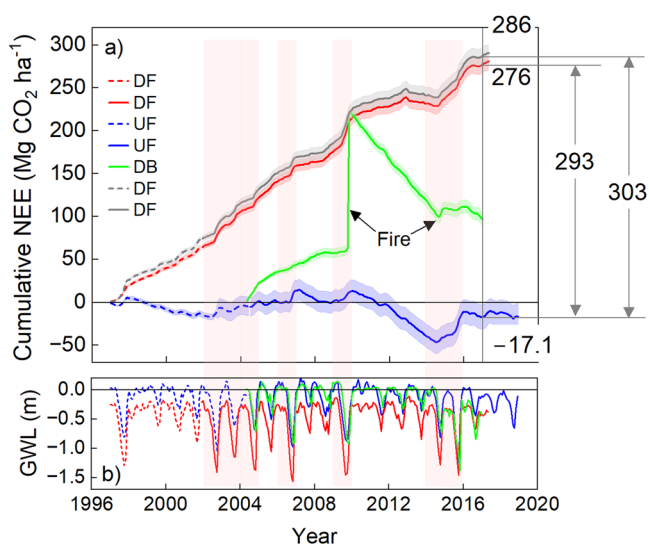


Fig. 4 | Cumulative change of monthly gap-filled NEE from canal excavation (January 1997) at the UF and DF and from the beginning of flux measurement (April 2004) at the DB, and monthly GWL variations at the three sites. a NEE and **b** GWL. Before flux measurement began in June 2004 at UF and October 2001 at DF, NEE was estimated monthly from estimated GWL (Supplementary Fig. 10) using a regression equation between NEE and GWL (Supplementary Fig. 11) (dashed line). For the DB, CO₂ emission through biomass burning (158 Mg CO₂ ha⁻¹ yr⁻¹) in 2009 is included. Shadows denote the 95% intervals. Pink bars denote the dry years. For DF, the initial emissions immediately after canal excavation were estimated alternatively (gray line). Over the 20 years until 2016, cumulative CO₂ emissions from the DF were 276 and 286 Mg CO₂ ha⁻¹ yr⁻¹, respectively, with and without considering initial large emissions, whereas that from the UF was -17.1 Mg CO₂ ha⁻¹ yr⁻¹ (a small CO₂ sink).

canopy conditions of the DF before the canal excavation are unknown, the lower LAI could have been caused by higher mortality, which were probably caused by long-term GWL lowering⁴². The mortality of DF increased from 1.61% in 2014 to 6.11% in 2015 owing to severe drought and then further increased to 9.66% in 2016 owing to the after-effects of the drought, resulting in a decrease in biomass (Supplementary Table 3).

The cumulative NEE (net CO₂ emissions) of the DF over 20 years after canal excavation until 2016 was 286 and 276 Mg CO₂ ha⁻¹ (Fig. 4), respectively, with and without considering initial large CO₂ emissions (Methods); cumulative emissions increased by 3.6% with the initial large emissions. Compared to the UF (-17.1 Mg CO₂ ha⁻¹), the net effect of drainage on annual CO₂ emissions was estimated to be 15.2 Mg CO₂ ha⁻¹ yr⁻¹ over the 20 years (Table 1).

Controlling factors

The ENSO droughts lowered the mean annual GWL by 0.22 m and changed the undrained UF from a CO₂ sink (Normal: -9.52 Mg CO₂ ha⁻¹ yr⁻¹) to a source (Dry: 13.1 Mg CO₂ ha⁻¹ yr⁻¹). The additional CO₂ emissions due to the droughts (22.6 Mg CO₂ ha⁻¹ yr⁻¹) resulted from a water deficit (17.6 Mg CO₂ ha⁻¹ yr⁻¹) and human-induced smoke haze (5.04 Mg CO₂ ha⁻¹ yr⁻¹) (Table 1). Between 2005 and 2016, excluding the wet years of 2010 and 2016, the mean annual additional emissions were calculated to be 7.04 Mg CO₂ ha⁻¹ yr⁻¹ from a water deficit and 2.02 Mg CO₂ ha⁻¹ yr⁻¹ from haze, considering the occurrence frequency of dry years (four of 10 years). Over the 20 years, a large canal lowered the GWL at the DF by 0.32 m on average compared to the UF. As a result, additional CO₂ was emitted at an annual rate of 15.2 Mg CO₂ ha⁻¹ yr⁻¹ (Table 1). However, the inter-site GWL difference decreased with time (Supplementary Fig. 7), resulting in a decrease in the RE at the DF (Supplementary Fig. 8). A large amount of CO₂ (158 Mg CO₂ ha⁻¹ yr⁻¹) was emitted during a fire in 2009 from the repeatedly burned DB²¹. After the 2009 fire, the DB changed drastically from

Table 1 | Mean annual NEE of the three sites and additional CO₂ emissions due to disturbances

a) Mean annual NEE and groundwater level (GWL) (mean ± 1 standard deviation)								
	Mean annual gap-filled NEE (Mg CO ₂ ha ⁻¹ yr ⁻¹)				GWL (m)			
	1997–2016	2005–2016			1997–2016	2005–2016		
		Weighted average ^a	Normal ^b	Dry ^c		All ^a	Normal ^b	Dry ^c
UF	-0.86 ± 10.9	-0.47 ± 14.8	-9.52 ± 6.93	13.1 ± 12.9	-0.16 ± 0.12	-0.15 ± 0.13	-0.08 ± 0.05	-0.30 ± 0.07
DF1 ^d	13.8 ± 9.45	13.5 ± 13.0	7.43 ± 8.76	22.5 ± 14.2	-0.48 ± 0.13	-0.46 ± 0.13	-0.40 ± 0.06	-0.62 ± 0.06
DF2 ^e	14.3 ± 9.75							
DB	N/A	12.0 ± 56.1 ^f	-7.78 ± 18.4	41.7 ± 83.2 ^f	N/A	-0.17 ± 0.19	-0.05 ± 0.03	-0.33 ± 0.17

b) Additional CO ₂ emissions (mean ± 1 standard deviation)				
	Additional CO ₂ emissions (Mg CO ₂ ha ⁻¹ yr ⁻¹)			
	1997–2016	2005–2016		
		Weighted average ^a	Normal ^b	Dry ^c
Drought_all ^g	N/A	9.06	N/A	22.6 ± 14.6
Drought_water ^h	N/A	7.04	N/A	17.6 ± 15.2
Drought_haze ⁱ	N/A	2.02	N/A	5.04 ± 3.99
Drainage1 ^j	14.7 ± 6.28	13.9 ± 8.85	16.9 ± 5.82	9.41 ± 11.1
Drainage2 ^k	15.2 ± 6.43			
Burning ^l	N/A	12.5 ± 51.2	1.73 ± 13.7	28.6 ± 84.2

^aWeighted average of the normal and dry years for 10 years, excluding the wet years of 2010 and 2016.

^b2005, 2007, 2008, 2011, 2012, and 2013.

^c2006, 2009, 2014, and 2015.

^dFor 1997–2001, monthly NEE was calculated from GWL using a relationship for DF (Supplementary Fig. 11).

^eFor 1997–2001, monthly NEE was calculated from GWL using a relationship for UF (Supplementary Fig. 11).

^fIncluding fire emissions.

^gDifference in annual NEE between the normal and dry years (Dry – Normal) at the UF. The sum of “Drought_water” and “Drought_haze”.

^hEmissions by a water deficit. Residual between “Drought” and “Drought_haze”

ⁱUptake decrease by smoke haze.

^jDifference in annual NEE between the UF and DF1 (DF1 – UF).

^kDifference in annual NEE between the UF and DF2 (DF2 – UF).

^lDifference in annual NEE between the UF and DB (DB – UF).

a continuous CO₂ source to a considerable sink (Fig. 4). The drastic change would have been caused by a large decrease of decomposition materials (plant debris) on the ground by burning and a large increase in GPP due to a rapid vegetation growth after the fire. However, the sink capacity is insufficient to recover large amounts of fire emissions²¹. Compared over the common period, the impact of drainage was 1.6 times greater than that of drought and almost equivalent to that of repeated burning (Table 1).

The mean annual NEE values of the UF and DF were -1.00 ± 13.2 Mg CO₂ ha⁻¹ yr⁻¹ (2005–2017) and 14.2 ± 10.9 Mg CO₂ ha⁻¹ yr⁻¹ (2002–2016), respectively (Supplementary Table 1). When a fluvial carbon loss of approximately 3 Mg CO₂ ha⁻¹ yr⁻¹ is added⁴³, the annual net CO₂ emissions were similar to the IPCC Tier 1 EF_{CO2} of 0 Mg CO₂ ha⁻¹ yr⁻¹ for “tropical rewetted organic soils” and 19.4 Mg CO₂ ha⁻¹ yr⁻¹ for “tropical forest land and cleared forest land (shrubland), drained”²⁷, respectively, despite different approaches (eddy covariance vs. chamber) and materials (ecosystem vs. only soil). Although CO₂ emissions depend on GWL and vary inter-annually, the IPCC EF_{CO2} might be usable to approximate the decadal mean ecosystem-scale net CO₂ emissions (NEE) of the PSF.

Annual NEE of PSFs increases as mean annual GWL decreases according to a single line (Fig. 2), as well as in northern peatlands²⁷. The slope of the line (-63.0) was very similar to that reported in a previous study (-64.65)⁹. The linear relationship based on long-term multipoint data was practical and robust for predicting the annual NEE of Southeast Asia’s PSFs because the data covered the main regions of peat distribution (Central Kalimantan, Riau, and Sarawak)¹ and included intact and drained (degraded) PSFs. The relationship indicates that every 10 cm decrease in mean annual GWL increases annual NEE by 6.30 Mg CO₂ ha⁻¹ yr⁻¹. Moreover, annual NEE would become zero at GWL of -0.18 m. The areas of pristine and degraded PSFs in Indonesia² were estimated to be 0.86 and 3.00 Mha in

2015. Under the assumption that the degraded PSF is drained⁵, the annual CO₂ emissions from all PSFs were calculated at 37.1 and 90.6 Tg CO₂ yr⁻¹ over Indonesia in the normal and dry years, respectively, using the mean annual GWL of the UF and DF (Table 1). The annual emissions in the normal and dry years account for 5.4% and 13.1% of Indonesia’s fossil fuel CO₂ emission in 2022 (692 Tg CO₂ yr⁻¹)⁴⁴, respectively. Overall, drought-induced GWL lowering increases CO₂ emissions from PSFs by a factor of 2.44 ($=90.6/37.1$); the large interannual variation potentially contributes to the positive effect of tropical drought on the atmospheric CO₂ growth rate^{45,46}. In Sumatra and Kalimantan (Indonesian Borneo), precipitation in the dry season is predicted to decrease under global warming, linking to sea surface temperature variability over the equatorial Pacific⁴⁷. Therefore, the GWL in PSFs would decrease in the future, potentially resulting in an increase in peat decomposition at a rate of 2.43 Tg CO₂ yr⁻¹ per every centimeter lowering of the mean annual GWL over Indonesia (3.86 Mha). In contrast, 10 cm rewetting of degraded PSF (3.00 Mha) can decrease CO₂ emissions by 19 Tg CO₂ yr⁻¹.

Methods

Study site

The CO₂ balance was measured at three peat swamp forest sites with different degrees of degradation: an almost undrained forest (UF), severely drained forest (DF), and repeatedly burned forest (DB)^{17,32,48}. The study sites were located within 15 km on tropical peat near Palangkaraya, Central Kalimantan, Indonesia (Supplementary Fig. 1). The UF site (2.32° S, 113.90° E) was in a National Park designated in 2006 but was selectively logged until the late 1990s. In addition, the site was slightly drained by small ditches made for logging; however, the shallow ditches were mostly buried naturally⁴⁹. The DF site (2.35° S, 114.04° E) was severely drained by a large

canal system (originally approximately 25 m width \times 3.5–4.5 m depth) constructed in 1996–1997 as part of the Mega Rice Project (MRP) infrastructure⁵⁰ (Supplementary Fig. 1), and was selectively logged until the end of the 1990s. The DB site (2.34° S, 114.04° E) (Supplementary Fig. 1) was located across the large canal and repeatedly burned during the El Niño years of 1997 (stand replacing), 2002 (peat burning), 2009 (moderate burning), and 2014 (light burning), and was drained further by a small ditch (approximately 1.5 m width) constructed in 2014 for plantation development²¹. Over the experimental period, canopy heights increased from 23 to 25 m and 26 to 28 m in the UF and DF, respectively. At the DB, the canopy increased from approximately 0.2 m in 2004 to 2 m in 2016 with a rapid decrease due to the 2009 fire²¹. The peat depths were 2–3 m, approximately 3 m, and approximately 4 m at the UF, DF, and DB, respectively. From 2002 to 2018, the mean annual precipitation was 2557 ± 432 mm yr⁻¹ (mean \pm 1 standard deviation (SD)), with a monthly maximum of 320 ± 108 mm month⁻¹ in December and a monthly minimum of 79 ± 76 mm month⁻¹ in August. In the same period, the mean annual air temperature at the tower top was 26.2 ± 0.27 °C with a small seasonal variation between 25.9 ± 0.34 °C in December and 26.8 ± 0.46 °C in May.

Flux and environmental measurement

The eddy fluxes of CO₂, sensible heat (H), and latent heat (LE) were measured using the eddy covariance technique on towers at three sites with a sonic anemometer-thermometer (CSAT3; Campbell Scientific Inc., Logan, UT, USA) and an open-path CO₂/H₂O analyzer (LI7500; Li-cor Inc., Lincoln, NE, USA)^{17,21,48} between July 2004 and August 2018 at the UF, November 2001 and June 2017 at the DF, and April 2004 and October 2016 at the DB. Measurement heights were 36.5 m at the UF and 41.3 m at the DF. At the DB, the height increased three times from 3.0 m to 13.6 m following tree growth. The CO₂ storage change in the space under the flux sensors was calculated from the vertical profile of the CO₂ concentration measured using a closed-path CO₂ analyzer (LI800 or LI820; Li-cor Inc.)^{17,21}. Shortwave radiation, net radiation (R_n), photosynthetic photon flux density (PPFD), air temperature, and relative humidity were also measured. Groundwater level (GWL) was measured at a hollow position at each site. The diffuse shortwave radiation fraction was calculated from the atmospheric clearness index, which is the ratio of downward shortwave radiation at the tower top to extra-terrestrial solar radiation around midday (10–14 h)²². The environmental measurements were extended to December 2019 and January 2017 at the UF and DB, respectively.

Flux calculation, quality control, gap-filling, and partitioning

The half-hourly eddy CO₂ flux was calculated using the Flux Calculator software⁵¹ with the same corrections as in our previous study²¹. Flux data were excluded to avoid flow distortion when the wind flowed from the tower direction¹⁷. Flux data were also excluded when it was rainy. A stationarity test was conducted to control the data quality^{21,52}, and the net ecosystem CO₂ exchange (NEE) was calculated as the sum of the eddy CO₂ flux and CO₂ storage change.

To exclude underestimated nighttime NEE caused by calm weather conditions, the change-point method was applied annually to determine the thresholds⁵³. Nighttime (PPFD < 20 $\mu\text{mol m}^{-2} \text{s}^{-1}$) NEE data, which is equivalent to ecosystem respiration (RE), were sorted by GWL and binned into quarters. Each binned dataset was further sorted by the SD of the vertical wind speed (σ_w) and binned again into equal-sized 50 groups. Using the 50 datasets, the change point (threshold) was determined for each of the four GWL ranges, and the four change points were then averaged as an annual threshold. If σ_w was lower than the threshold value, the measured NEE was excluded. Although the air temperature was originally used⁵³, GWL was used in this study because it mainly controls RE in tropical peatlands¹⁷. In addition, σ_w was used instead of the friction velocity (u^*) because the change points were determined more robustly using σ_w than u^* ⁵⁴. The annual σ_w thresholds were 0.305 ± 0.073 and 0.304 ± 0.050 m s⁻¹ (mean \pm 1 SD) at the UF and DF, respectively. At DB, the thresholds were

determined to be 0.152 m s⁻¹ for 2015 and 0.144 m s⁻¹ for 2016, but we failed to determine change points until 2015, when the vegetation was still short. Thus, σ_w thresholds were not applied to the DB during or before 2014.

Outliers included in the surviving data were further screened using the Smirnov–Grubbs rejection test ($\alpha = 0.05$) separately for daytime (PPFD ≥ 20 mol m⁻² s⁻¹) and nighttime annually. Finally, including data gaps due to power problems and system malfunctions, the annual survival fractions of half-hourly NEE data were $44.8 \pm 10.1\%$ (UF), $38.8 \pm 15.4\%$ (DF), and $56.6 \pm 18.1\%$ (DB) for daytime and $5.8 \pm 1.8\%$ (UF), $5.2 \pm 5.6\%$ (DF), and $40.2 \pm 12.5\%$ (DB) for nighttime; the higher nighttime fraction at DB was due to no application of σ_w thresholds until 2015. To fill these data gaps, the marginal distribution sampling method (MDS)⁵⁵ was applied to the half-hourly daytime NEE using PPFD, vapor pressure deficit (VPD), air temperature, and GWL as environmental variables. However, nighttime NEE or nighttime RE was gap-filled from only GWL using the look-up table method⁵⁶. Half-hourly nighttime RE data were sorted by GWL and equally binned into seven groups. The look-up table, consisting of seven mean RE against the GWL, was created annually. The simple look-up table method was selected instead of the MDS method because the MDS method provided unstable outputs owing to the low fraction of surviving data. Half-hourly daytime RE was estimated from GWL using annual look-up tables for nighttime RE, and gross primary production (GPP) was calculated as the difference between daytime RE and NEE (GPP = RE – NEE). Gap-filled half-hourly data of CO₂ flux, meteorology, and groundwater level are available in a repository⁵⁷.

The uncertainty in the annual NEE summation caused by random errors and gap filling was evaluated using the 24-h differencing approach^{58,59}. Difference between two NEE measurements exactly 24 h apart was calculated as a random error, if environmental conditions were similar. Details of the methods are given in our previous study²¹.

Biometric measurement

Four circular plots with a radius of 21 m were established in cardinal directions, 50 m from the tower at each site (Supplementary Fig. 9). Three concentric subplots (SPs) of different radii were embedded in each plot. The radii of SP1, SP2, and SP3 were 7 m (154 m²), 14 m (616 m²), and 21 m (1385 m²), respectively. Within the SPs, all trees with diameters (DBH) at breast height (1.3 m) of 3–10, 10–20, and >20 cm were tagged for tree surveys in SP1, SP2, and SP3, respectively, at the UF and DF in September 2013, and tree species and DBH were recorded. At the DB, targeted DBHs were 3–5, 5–10, and >10 cm, respectively, but trees with a DBH > 10 cm were not found. In the UF and DF, 53 and 62 tree species were identified, respectively. The top five dominant species in the stem area were *Cratogeomys arborescens*, *Beilschmiedia madang*, *Pampaning Bitik*, *Combretocarpus rotundatus* (Tumih), and *Neoscortechinia kingii* in the UF, accounting for 32.1% of the total stem area, and these five species accounted for 22.1% at DF. However, in the DB, only *Combretocarpus rotundatus* dominated the tree species at 98.5%. Simultaneously, four litter traps with an opening area of 1.0 m² were installed at a height of 1 m in each SP2, totaling 16 traps at each site. In addition, four rectangular plots (4 \times 10 m) were established near the circular plots at the DB to estimate the biomass and leaf area index (LAI) of the fern plants (*Stenochlaena*, *Blechnum*, and *Lygodium* spp.). Each rectangular plot was divided into ten subplots measuring 2 m \times 2 m.

The DBH of all tagged trees was measured annually from September 2013 to 2016. From the DBH, aboveground biomass (stems, branches, twigs, and leaves) (AGB, kg tree⁻¹), belowground biomass (coarse roots) (BGB, kg tree⁻¹), and leaf dry mass (LDM, kg tree⁻¹) were calculated using allometric equations⁶⁰, which were determined for tropical peat swamp forests in Sumatra, and then summed for each plot. The LDM was converted to LAI using a stand-level leaf mass per unit leaf area (LMA: total leaf mass/LAI) of 1.8 Mg ha⁻¹, which was determined from a field survey in a UF forest⁶¹.

Litterfall, including branches, twigs, leaves, seeds, fruits, and flowers, was collected monthly from litter traps and dried at 80 °C for 48 h. Litter sampling was conducted from October 2013 to September 2014 at DB,

December 2015 at DF, and September 2016 at UF. Litter traps at DB were burned during the 2014 fire. The annual net primary production (NPP) of trees was calculated as the sum of the annual change in total tree biomass (AGB + BGB) and the annual litter fall. Biomass and litterfall (dry mass) were converted to carbon using a factor of 0.464⁶². Because fine root NPP, which was not measured, contributed to 21% of the total NPP on average for the mature tropical rainforest in Amazonia⁶³, the annual NPP was corrected by adding fine root NPP using a factor of 1.27 (=1/(1 - 0.21)).

The height and vegetation coverage of fern plants were measured nondestructively in each rectangular subplot at the DB. AGB and LAI were estimated using linear (AGB, $R^2 = 0.88$) and power (LAI, $R^2 = 0.88$) relationships, respectively, with the product of plant height and vegetation coverage. Measurements were conducted monthly from October 2013 to September 2014, immediately before the 2014 fire.

The results of biometric measurement are summarized in Supplementary Table 3.

Environmental response of gross primary production

The response of GPP ($\mu\text{mol m}^{-2} \text{s}^{-1}$) to PPFD ($\mu\text{mol m}^{-2} \text{s}^{-1}$) was examined using the following non-rectangular hyperbola for half-hourly GPP data partitioned from measured daytime NEE (not gap-filled), considering VPD dependence²⁸:

$$GPP = \frac{\alpha \cdot PPFD + GPP_{\max} - \sqrt{(\alpha \cdot PPFD + GPP_{\max})^2 - 4 \cdot \alpha \cdot GPP_{\max} \cdot \theta \cdot PPFD}}{2 \cdot \theta} \quad (1)$$

$$GPP_{\max} = GPP_0 \cdot \exp\{-k \cdot (VPD - VPD_0)\}, \text{ if } VPD > VPD_0 \quad (2)$$

$$GPP_{\max} = GPP_0, \text{ if } VPD \leq VPD_0 \quad (3)$$

where α is the initial slope of the curve ($\mu\text{mol CO}_2 \mu\text{mol photon}^{-1}$), GPP_{\max} is the light-saturated GPP, VPD_0 is the VPD threshold (kPa), GPP_0 is the GPP_{\max} without the VPD limitation ($VPD \leq VPD_0$), k is the coefficient of the VPD response, and θ is the curvature. VPD_0 was set to be 1.0 kPa at all sites²⁸. The parameters of α , GPP_0 , k , and θ were determined by curve fitting using OriginPro 2021b software (Origin Lab Corporation, Northampton, MA, USA).

When we simulated the effect of haze smoke on GPP at the UF (Fig. 3), GPP_0 in Eqs. (2) and (3) was replaced with $GPP_{0,GWL}$ because GPP_0 showed a decreasing tendency at low GWL (Supplementary Fig. 4).

$$GPP_{0,GWL} = GPP_0 \cdot [0.461 \cdot (GWL + 0.7) + 1], \text{ if } GWL < -0.7m \quad (4)$$

$$GPP_{0,GWL} = GPP_0, \text{ if } GWL \geq -0.7m \quad (5)$$

Surface conductance and its response to vapor pressure deficit

The bulk surface conductance to water vapor (G_s , m s^{-1}) was calculated backward from the Penman–Monteith equation⁶⁴ by replacing the available energy ($R_n - G$) with the eddy energy flux ($H + IE$) because the soil heat flux (G) was not measured⁴⁸.

$$\frac{1}{G_s} = \frac{1}{G_a} \left[\frac{\varepsilon \cdot (R_n - G) + \rho \cdot C_p \cdot G_a \cdot \frac{VPD}{\gamma}}{IE} - \varepsilon - 1 \right] \quad (6)$$

G_a stands for the bulk aerodynamic conductance (m s^{-1}), ε signifies s / γ , s represents the slope of the relationship between saturation vapor pressure and temperature (kPa K^{-1}), γ denotes the psychrometric constant (0.067 kPa K^{-1}), ρ represents the air density (kg m^{-3}), and C_p denotes the specific heat of air at constant pressure ($1007 \text{ J kg}^{-1} \text{ K}^{-1}$). The

G_a was calculated using the following equation⁶⁵ as:

$$G_a = \left[\frac{2}{\kappa \cdot u^*} \left(\frac{dh}{dv} \right)^{\frac{3}{2}} + \frac{u}{u^{*2}} \right]^{-1} \quad (7)$$

where κ is the von Karman constant ($=0.4$), u^* denotes the friction velocity (m s^{-1}), dh represents thermal diffusivity, dv stands for the molecular diffusivity of water vapor, and u signifies mean wind velocity (m s^{-1}). The ratio of dh to dv was set as 0.89⁶⁵. G_s was only calculated when there was no antecedent precipitation within five hours to avoid the effects of canopy evaporation. In addition, to avoid the effect of light intensity on stomatal conductance, G_s was calculated only when the PPFD was higher than $1000 \mu\text{mol m}^{-2} \text{s}^{-1}$. The units of G_s were converted to $\text{mmol m}^{-2} \text{s}^{-1}$. Because the canopy was closed at the UF and DF, dry G_s was almost equivalent to stomatal conductance, whereas ground surface evaporation was incorporated into G_s at the DB because of its open canopy.

The relationship between G_s and VPD was examined using^{29,30}:

$$G_s = G_{s,\text{ref}} [1 - m \cdot \ln(VPD)] \quad (8)$$

where $G_{s,\text{ref}}$ is the reference G_s ($\text{mmol m}^{-2} \text{s}^{-1}$) at $VPD = 1.0 \text{ kPa}$, and m is the sensitivity of G_s to VPD. The parameters $G_{s,\text{ref}}$ and m were determined by curve fitting using the OriginPro 2021b software (OriginLab Corporation).

Cumulative net ecosystem CO₂ exchange after canal construction

To calculate the cumulative CO₂ emissions from 1997 after canal construction near the DF, the NEE was estimated from the GWL until the flux measurement began. First, monthly mean GWLs at the UF and DF were estimated from GWL data measured since 1993 at the Takahashi site⁴⁹ 460 m from the UF using linear relationships (Supplementary Fig. 10), and the monthly mean NEE was calculated from the estimated GWL using linear relationships between NEE and GWL at each site (Supplementary Fig. 11). The 95% confidence intervals of cumulative NEE were calculated according to the law of error propagation. However, this method potentially underestimates large CO₂ emissions immediately after drainage began^{12,13}. Therefore, monthly NEE before flux measurement at the DF was further estimated from the estimated DF's GWL using the linear relationship between NEE and GWL at the undrained UF (Supplementary Fig. 11).

Classification of years by precipitation patterns

To examine the effect of drought mainly caused by the ENSO, the years from 2002 to 2018 were classified into normal, dry, and wet years using the dry period length (DPL), which is defined as the number of days with a 30-day moving precipitation total smaller than 100 mm^{26} . Over the 17 years, DPL ranged from 0 days in 2010 to 166 days in 2009, with a mean of 85 ± 46 days (± 1 SD). In this study, the thresholds were determined as follows: dry >100 , normal >40 , and wet ≤ 40 days. As a result, seven years (2005, 2007, 2008, 2011, 2012, 2013, and 2018) were normal, seven years (2002, 2003, 2004, 2006, 2009, 2014, and 2015) were dry, and three years (2010, 2016, and 2017) were wet (Supplementary Table 1).

Monthly burned fraction (BF) data around the study sites³² (Global Fire Emission Database; <https://globalfireatlas.spages.com/data/>) showed that fires occurred in the dry season almost every year, except for wet years (Supplementary Fig. 2). The BF increased in the dry years following sharp negative GWL peaks. The resultant dense smoke or haze decreased the PPFD and increased the diffuse radiation fraction, especially in 2002, 2006, 2009, 2014, and 2015 (Supplementary Fig. 2).

Data availability

The CO₂ flux, meteorology, and groundwater level data that support the findings of this study are available on figshare [<https://figshare.com/s/6ae20137486d0a6f62>].

Received: 25 September 2023; Accepted: 12 April 2024;
Published online: 25 April 2024

References

- Page, S. et al. Anthropogenic impacts on lowland tropical peatland biogeochemistry. *Nat. Rev. Earth Environ.* **3**, 426–443 (2022).
- Miettinen, J., Shi, C. & Liew, S. C. Land cover distribution in the peatlands of Peninsular Malaysia, Sumatra and Borneo in 2015 with changes since 1990. *Global Ecol. Conserv.* **6**, 67–78 (2016).
- Dadap, N. C. et al. Drainage Canals in Southeast Asian Peatlands Increase Carbon Emissions. *AGU Adv.* **2** <https://doi.org/10.1029/2020av000321> (2021).
- Wakhid, N., Hirano, T., Okimoto, Y., Nurzakiah, S. & Nursyamsi, D. Soil carbon dioxide emissions from a rubber plantation on tropical peat. *Sci. Total Environ.* **581**, 857–865 (2017).
- Miettinen, J., Hooijer, A., Vernimmen, R., Liew, S. C. & Page, S. E. From carbon sink to carbon source: extensive peat oxidation in insular Southeast Asia since 1990. *Environ. Res. Lett.* **12**, 024014 (2017).
- Wijedasa, L. S. et al. Carbon emissions from South-East Asian peatlands will increase despite emission-reduction schemes. *Glob. Chang. Biol.* **24**, 4598–4613 (2018).
- Hiraishi, T. et al. (eds.) 2013 Supplement to the 2006 IPCC Guidelines for National Greenhouse Gas Inventories: Wetlands. (IPCC, Switzerland, 2014).
- Shiraishi, T., Hirata, R. & Hirano, T. New Inventories of Global Carbon Dioxide Emissions through Biomass Burning in 2001–2020. *Remote Sens.* **13** <https://doi.org/10.3390/rs13101914> (2021).
- Deshmukh, C. S. et al. Net greenhouse gas balance of fibre wood plantation on peat in Indonesia. *Nature* **616**, 740–746 (2023).
- Hirano, T., Kusin, K., Limin, S. & Osaki, M. Carbon dioxide emissions through oxidative peat decomposition on a burnt tropical peatland. *Glob. Chang. Biol.* **20**, 555–565 (2014).
- Ishikura, K. et al. Carbon Dioxide and Methane Emissions from Peat Soil in an Undrained Tropical Peat Swamp Forest. *Ecosystems* **22**, 1852–1868 (2019).
- Hooijer, A. et al. Current and future CO₂ emissions from drained peatlands in Southeast Asia. *Biogeosciences* **7**, 1505–1514 (2010).
- Swails, E., Hergoualc'h, K., Deng, J., Froking, S. & Novita, N. How can process-based modeling improve peat CO₂ and N₂O emission factors for oil palm plantations? *Sci. Total Environ.* **839**, 156153 (2022).
- Könönen, M. et al. Deforested and drained tropical peatland sites show poorer peat substrate quality and lower microbial biomass and activity than unmanaged swamp forest. *Soil Biol. Biochem.* **123**, 229–241 (2018).
- Alsepan, G. & Minobe, S. Relations between Interannual Variability of Regional-Scale Indonesian Precipitation and Large-Scale Climate Modes during 1960–2007. *J. Clim.* **33**, 5271–5291 (2020).
- Cai, W. et al. Changing El Niño–Southern Oscillation in a warming climate. *Nat. Rev. Earth Environ.* **2**, 628–644 (2021).
- Hirano, T. et al. Effects of disturbances on the carbon balance of tropical peat swamp forests. *Global Change Biol.* **18**, 3410–3422 (2012).
- Ohkubo, S., Hirano, T. & Kusin, K. Influence of disturbance on transpiration and evaporation in tropical peat swamp forests. *J. Hydrol.* **620** <https://doi.org/10.1016/j.jhydrol.2023.129523> (2023).
- Page, S. E. & Hooijer, A. In the line of fire: the peatlands of Southeast Asia. *Philos. Trans. R Soc. Lond. B. Biol. Sci.* **371**, 20150176 (2016).
- Page, S. E. et al. The amount of carbon released from peat and forest fires in Indonesia during 1997. *Nature* **420**, 61–65 (2002).
- Ohkubo, S., Hirano, T. & Kusin, K. Assessing the carbon dioxide balance of a degraded tropical peat swamp forest following multiple fire events of different intensities. *Agric. Forest Meteorol.* **306** <https://doi.org/10.1016/j.agrformet.2021.108448> (2021).
- Marpaung, F. & Hirano, T. Environmental dependence and seasonal variation of diffuse solar radiation in tropical peatland. *J. Agric. Meteorol.* **70**, 223–232 (2014).
- Stiegler, C. et al. El Niño–Southern Oscillation (ENSO) event reduces CO₂ uptake of an Indonesian oil palm plantation. *Biogeosciences* **16**, 2873–2890 (2019).
- Lewis, S. L. Tropical forests and the changing earth system. *Philos. Trans. R. Soc. Lond. B Biol. Sci.* **361**, 195–210 (2006).
- Kiew, F. et al. CO₂ balance of a secondary tropical peat swamp forest in Sarawak, Malaysia. *Agric. Forest Meteorol.* **248**, 494–501 (2018).
- Kume, T. et al. Ten-year evapotranspiration estimates in a Bornean tropical rainforest. *Agric. Forest Meteorol.* **151**, 1183–1192 (2011).
- Evans, C. D. et al. Overriding water table control on managed peatland greenhouse gas emissions. *Nature* **593**, 548–552 (2021).
- Lasslop, G. et al. Separation of net ecosystem exchange into assimilation and respiration using a light response curve approach: critical issues and global evaluation. *Global Change Biol.* **16**, 187–208 (2010).
- Novick, K. A. et al. The increasing importance of atmospheric demand for ecosystem water and carbon fluxes. *Nat. Clim. Change* **6**, 1023–1027 (2016).
- Oren, R. et al. Survey and synthesis of intra- and interspecific variation in stomatal sensitivity to vapour pressure deficit. *Plant Cell Environ.* **22**, 1515–1526 (1999).
- Gaveau, D. L. et al. Major atmospheric emissions from peat fires in Southeast Asia during non-drought years: evidence from the 2013 Sumatran fires. *Sci. Rep.* **4**, 6112 (2014).
- Ohkubo, S., Hirano, T. & Kusin, K. Influence of disturbances and environmental changes on albedo in tropical peat ecosystems. *Agric. Forest Meteorol.* **301–302** <https://doi.org/10.1016/j.agrformet.2021.108348> (2021).
- Kobayashi, H., Matsunaga, T. & Hoyano, A. Net primary production in Southeast Asia following a large reduction in photosynthetically active radiation owing to smoke. *Geophys. Res. Lett.* **32** <https://doi.org/10.1029/2004gl021704> (2005).
- Knohl, A. & Baldocchi, D. D. Effects of diffuse radiation on canopy gas exchange processes in a forest ecosystem. *J. Geophys. Res.* **113** <https://doi.org/10.1029/2007jg000663> (2008).
- Oliveira, P. H. F. et al. The effects of biomass burning aerosols and clouds on the CO₂ flux in Amazonia. *Tellus Ser. B Chem. Phys. Meteorol.* **59**, 338–349 (2007).
- Konecny, K. et al. Variable carbon losses from recurrent fires in drained tropical peatlands. *Glob. Chang. Biol.* **22**, 1469–1480 (2016).
- Sundari, S., Hirano, T., Yamada, H., Kushin, K. & Limin, S. Effects of groundwater level on soil respiration in tropical peat swamp forests. *J. Agric. Meteorol.* **68**, 121–134 (2012).
- Itoh, M., Okimoto, Y., Hirano, T. & Kusin, K. Factors affecting oxidative peat decomposition due to land use in tropical peat swamp forests in Indonesia. *Sci. Total Environ.* **609**, 906–915 (2017).
- Evans, C. D. et al. Rates and spatial variability of peat subsidence in Acacia plantation and forest landscapes in Sumatra, Indonesia. *Geoderma* **338**, 410–421 (2019).
- Tauc, F., Houle, D., Dupuch, A., Doyon, F. & Maheu, A. Microtopographic refugia against drought in temperate forests: Lower water availability but more extensive fine root system in mounds than in pits. *Forest Ecol. Manag.* **476** <https://doi.org/10.1016/j.foreco.2020.118439> (2020).
- Schuldts, B. et al. Change in hydraulic properties and leaf traits in a tall rainforest tree species subjected to long-term throughfall exclusion in the perhumid tropics. *Biogeosciences* **8**, 2179–2194 (2011).
- Gessler, A., Schaub, M. & McDowell, N. G. The role of nutrients in drought-induced tree mortality and recovery. *New Phytol.* **214**, 513–520 (2017).
- Moore, S. et al. Deep instability of deforested tropical peatlands revealed by fluvial organic carbon fluxes. *Nature* **493**, 660–663 (2013).

44. Crippa, M. et al. *GHG emissions of all world countries*, 263 (Luxembourg, 2023).
45. Liu, L. et al. Increasingly negative tropical water-interannual CO₂ growth rate coupling. *Nature* **618**, 755–760 (2023).
46. Luo, X. & Keenan, T. F. Tropical extreme droughts drive long-term increase in atmospheric CO₂ growth rate variability. *Nat. Commun.* **13**, 1193 (2022).
47. Ghosh, R. & Shepherd, T. G. Storylines of maritime continent dry period precipitation changes under global warming. *Environ. Res. Lett.* **18**, 034017 (2023).
48. Hirano, T., Kusin, K., Limin, S. & Osaki, M. Evapotranspiration of tropical peat swamp forests. *Global Change Biol.* **21**, 1914–1927 (2015).
49. Sulaiman, A. et al. Peatland groundwater level in the Indonesian maritime continent as an alert for El Niño and moderate positive Indian Ocean dipole events. *Sci. Rep.* **13**, 939 (2023).
50. Page, S. et al. Restoration Ecology of Lowland Tropical Peatlands in Southeast Asia: Current Knowledge and Future Research Directions. *Ecosystems* **12**, 888–905 (2009).
51. Ueyama, M. et al. Influences of various calculation options on heat, water and carbon fluxes determined by open- and closed-path eddy covariance methods. *Tellus Ser. B Chem. Phys. Meteorol.* **64** <https://doi.org/10.3402/tellusb.v64i0.19048> (2012).
52. Foken, T. & Wichura, B. Tools for quality assessment of surface-based flux measurements. *Agric. Forest Meteorol.* **78**, 83–105 (1996).
53. Barr, A. G. et al. Use of change-point detection for friction-velocity threshold evaluation in eddy-covariance studies. *Agric. Forest Meteorol.* **171–172**, 31–45 (2013).
54. Acevedo, O. C. et al. Is friction velocity the most appropriate scale for correcting nocturnal carbon dioxide fluxes? *Agric. Forest Meteorol.* **149**, 1–10 (2009).
55. Reichstein, M. et al. On the separation of net ecosystem exchange into assimilation and ecosystem respiration: review and improved algorithm. *Global Change Biol.* **11**, 1424–1439 (2005).
56. Falge, E. et al. Gap filling strategies for long term energy flux data sets. *Agric. Forest Meteorol.* **107**, 71–77 (2001).
57. Hirano, T. *The CO₂ flux, meteorology, and groundwater level data*, <https://figshare.com/s/6aeef20137486d0a6f62> (2024).
58. Richardson, A. D. & Hollinger, D. Y. A method to estimate the additional uncertainty in gap-filled NEE resulting from long gaps in the CO₂ flux record. *Agric. Forest Meteorol.* **147**, 199–208 (2007).
59. Richardson, A. D. et al. A multi-site analysis of random error in tower-based measurements of carbon and energy fluxes. *Agric. Forest Meteorol.* **136**, 1–18 (2006).
60. Suwarna, U., Elias, Darusman, D. & Istomo, D. Estimation of total carbon stocks in soil and vegetation of tropical peat forest in Indonesia. *J. Manaj. Hutan Trop.* **18**, 118–128 (2012).
61. Miyamoto, K., Kohyama, T., Rahajoe, J., Mirmanto, E. & Simbolom, H. in *Tropical Peatland Ecosystems* (eds M. Osaki & N. Tsuji) 151–166 (Springer, 2016).
62. Murdiyarto, D. et al. *Carbon storage in mangrove and peatland ecosystems: A preliminary account from plots in Indonesia*, 35 (Bogor, Indonesia, 2009).
63. Malhi, Y. et al. Comprehensive assessment of carbon productivity, allocation and storage in three Amazonian forests. *Global Change Biol.* **15**, 1255–1274 (2009).
64. Monteith, J. L. Evaporation and the environment. *Symp. Soc. Exploratory Biol.* **19**, 205–234 (1965).
65. Humphreys, E. R. et al. Summer carbon dioxide and water vapor fluxes across a range of northern peatlands. *J. Geophys. Res.* **111** <https://doi.org/10.1029/2005jg000111> (2006).

Acknowledgements

We thank the late Dr. Suwido Limin for the site establishment and Drs. Yosuke Okimoto, Kiwamu Ishikura, and the staff of CIMTROP for their assistance in field work. This work was supported by JSPS Core University Program, JSPS KAKENHI Grant Numbers 13375011, 15255001, 18403001, 21255001, 25257401 and 19H05666, the JST-JICA Project (SATREPS) (Wild Fire and Carbon Management in Peat-Forest in Indonesia), Technology Development Fund (no. 2–1504) by the Environmental Restoration and Conservation Agency and the Ministry of the Environment, Japan, and Research Institute for Humanity and Nature (RIHN, Project No. 14200117).

Author contributions

Hirano conceived the study. Ohkubo and Sakabe completed flux data processing. Hirano, Itoh, and Kusin maintained the field system and collected data. Tsuzuki completed biometric measurement. Takahashi completed the long-term hydrological measurement. Osaki launched the field experiment of tropical peatlands in this area. Hirano conceived the paper and wrote the initial draft, to which all authors provided critical contribution.

Competing interests

The authors declare no competing interests.

Additional information

Supplementary information The online version contains supplementary material available at <https://doi.org/10.1038/s43247-024-01387-7>.

Correspondence and requests for materials should be addressed to Takashi Hirano.

Peer review information *Communications Earth & Environment* thanks Timothy Hill and the other, anonymous, reviewer(s) for their contribution to the peer review of this work. Primary Handling Editors: Huai Chen and Clare Davis. A peer review file is available.

Reprints and permissions information is available at <http://www.nature.com/reprints>

Publisher's note Springer Nature remains neutral with regard to jurisdictional claims in published maps and institutional affiliations.

Open Access This article is licensed under a Creative Commons Attribution 4.0 International License, which permits use, sharing, adaptation, distribution and reproduction in any medium or format, as long as you give appropriate credit to the original author(s) and the source, provide a link to the Creative Commons licence, and indicate if changes were made. The images or other third party material in this article are included in the article's Creative Commons licence, unless indicated otherwise in a credit line to the material. If material is not included in the article's Creative Commons licence and your intended use is not permitted by statutory regulation or exceeds the permitted use, you will need to obtain permission directly from the copyright holder. To view a copy of this licence, visit <http://creativecommons.org/licenses/by/4.0/>.

© The Author(s) 2024